Hindawi
Journal of Sensors
Volume 2017, Article ID 2190429, 6 pages
https://doi.org/10.1155/2017/2190429

Research Article

Investigations of Printed Flexible pH Sensing Materials Based on Graphene Platelets and Submicron RuO_2 Powders

Daniel Janczak,[1] Andrzej Peplowski,[1] Grzegorz Wroblewski,[1] Lukasz Gorski,[2] Elzbieta Zwierkowska,[3] and Malgorzata Jakubowska[1]

[1]*Institute of Metrology and Biomedical Engineering, Warsaw University of Technology, A. Boboli 8, 02-525 Warsaw, Poland*
[2]*Institute of Biotechnology, Warsaw University of Technology, Noakowskiego 3, 00-664 Warsaw, Poland*
[3]*Institute of Electronic Materials Technology, Wolczynska 133, 01-919 Warsaw, Poland*

Correspondence should be addressed to Malgorzata Jakubowska; maljakub@mchtr.pw.edu.pl

Received 5 December 2016; Revised 1 February 2017; Accepted 16 February 2017; Published 6 March 2017

Academic Editor: Sher Bahadar Khan

The paper describes the investigations of pH-sensitive materials for screen printed flexible pH sensors. The sensors were fully printed and consisted of three layers, conductive made of low temperature-curable silver paste, insulating made of UV-curable dielectric paste, and pH-sensitive made of developed graphene/ruthenium oxide pastes. Graphene and ruthenium oxide composites were prepared with different proportions of graphene nanoplatelets paste and submicron ruthenium dioxide. To perform functional measurements, particular testing sensors were fabricated on flexible polyester foil. Afterwards electrochemical potential measurements of fabricated devices were carried out. Sensors were also exposed to cyclic bending and the change of pH sensitivity before and after bending was described. Eventually, percolation threshold concerning the amount of ruthenium oxide in the pH-sensitive layer was designated and UV influence on the sensitivity was observed that together allow for optimization of sensors' fabrication costs.

1. Introduction

Printed electronics is a rapidly growing field of technology strongly investigated by both the research institutions and companies seeking for new products. Printed electronics has a lot of benefits such as easy processing without the need for vacuum, clean rooms, or high temperatures. The possibility of low temperature processing made this technology advisable for applications using flexible materials, such as polymer foils [1], papers [2], and fabrics [3]. Electronic devices may be fabricated with printing processes, such as screen printing [4], flexography [5], ink-jet printing [6], gravure [7], or pad printing [8] which are well known from graphics industry. Thanks to novel materials suitable for electronics there are vast possibilities of fabrication of functional printings, such as conductive [9], resistive [10], dielectric [11], or sensitive layers [12]. Those printable materials may be used for fabrication of electronic elements, such as conductive paths [13], antennas [14], capacitors [15], resistors [16], heaters [17], light sources [18], or diverse sensors [19].

Measuring the proton activity (pH) of environment is one of the basic chemical measurements required in various fields of human interest, like biotechnology [20], medicine [21], environmental science [22], water-support system monitoring [23], food safety [24], and many others. Apart from direct pH measurement, sensors detecting proton activity can be employed as a basis for modification, for example, with enzymes [25], nucleic acids [26], or microorganisms [27], yielding biosensors for even more applications. Given this need for sensing of pH and pH-affecting markers or reactions, improvement and development of appropriate production technologies is a relevant task for research. In this paper, authors present a printed electronics-based approach to fabrication of the pH-sensitive potentiometric electrodes. Pastes prepared for screen printing of the functional layer of the transceivers were based on the previously developed conductive graphene composites [28] with addition of the ruthenium (IV) oxide as the proton-sensitive phase, of which response mechanism was described in detail elsewhere [29, 30].

Briefly, after immersion of the metal oxide in the solution, protons and hydroxide ions are bound to the oxygen ions in the metal oxide crystal lattice and with the surface cations, respectively, resulting in covering the metal oxide surface with the hydroxyl groups. Then, exchange of the protons between the hydroxyl groups and the solution occurs and thus the electrical potential of the surface is determined by the H^+/OH^- ions balance in the solution [30–32]. There are also reports [33] on the pH-sensitive electrodes based on the mixture of the RuO_2 with another, chemically inert oxide, aimed at reduction of material costs derived from the RuO_2 expensiveness. In these works however, sensors' performance drop was reported.

Graphene also exhibits similar properties that allow for pH sensing, as described by Lei et al. [34] and Ang et al. [35]. H_3O^+ and OH^- ions from the solution are adsorbed on the graphene surface depending on the solution's pH. At the same time, graphene nanoplatelets (GNP) are much cheaper than RuO_2.

Based on these facts, successful implementation of graphene for pH sensors fabrication and reports on the binary metal oxide electrodes [36], authors investigated a possibility of employment of RuO_2/GNP nanocomposite for potential cost-effective pH sensor fabrication. Presented work was aimed at resulting in both pH sensing transceiver and satisfying utility requirements, such as production costs optimization, manufacturing process simplicity, and sensor's flexibility.

2. Materials and Methods

2.1. Materials. Poly(methyl methacrylate) (PMMA) with average molecular weight M_w = 350,000; diethylene glycol butyl ether acetate ≥99% pure; toluene ≥99.3% pure and citric acid 99% pure were purchased from Sigma-Aldrich. Ruthenium(IV) oxide Premion submicron powder with 74% Ru was acquired from Alfa Aesar (Germany). Sodium hydroxide was purchased from POCH S.A. (Poland).

Graphene nanoplatelets M-25 with 25 μm average diameter and typical surface area of 120 to 150 $m^2 \cdot g^{-1}$ were acquired from XG Sciences Inc. (USA). Silver paste L-121 based on silver microflakes was acquired from ITME (Poland). The insulating UV-curable 5018G and heat-curable 8155 pastes were bought from DuPont. Polyester (PET) foil Melinex 453 with a thickness of 100 μm was delivered by TEKRA (USA).

2.2. Preparation of Printing Pastes. Screen printing pastes for pH-sensitive layers were composed of PMMA polymer matrix, graphene nanoplatelets, and ruthenium oxide powders. Firstly 8 wt% PMMA resin was prepared by dissolving the PMMA granulate in diethylene glycol butyl ether by means of magnetic stirrer (48 hours in 60°C). Secondly, 12 wt% graphene nanoplatelets paste was prepared by adding the graphene platelets to the 8 wt% PMMA resin prepared earlier. Paste was rolled two times in the three-roll-mill with silicon carbide (SiC) rollers and 5 μm gap to obtain homogenous compositions without agglomerates. After receiving suitable graphene nanoplatelets paste, the paste was divided into 6 parts and final set of 6 different (10 wt%, 20 wt%, 30 wt%, 40 wt%, 50 wt%, and 60 wt%) compositions with ruthenium oxide was prepared according to Table 1. Also, RuO_2 paste was prepared by 40 wt% addition of RuO_2 to the 8 wt% PMMA resin. After adding appropriate amounts of RuO_2, each sample was rolled again with the three-roll-mill.

Table 1: Compositions of screen printing RuO_2/GNP/PMMA pastes for pH-sensitive layers.

Paste	RuO_2 content, wt%	Graphene paste 12 wt%, g	RuO_2, g
1	10	1.8	0.2
2	20	1.6	0.4
3	30	1.4	0.6
4	40	1.2	0.8
5	50	1.0	1.0
6	60	0.8	1.2

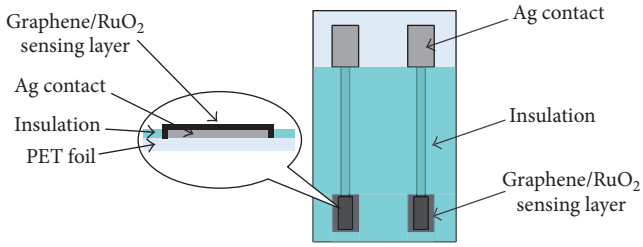

Figure 1: Schematic diagram of the sensor structure.

2.3. Fabrication of Sensors. Sensors were fabricated on the PET foil and consisted of three subsequently printed layers (as shown in Figure 1) made by means of Ami Presco 485 screen printer. Firstly, silver contacts and conductive paths were deposited with the use of commercially available silver screen printing paste (L-121). Secondly, pH-sensitive GNP/RuO_2 layers were printed prepared as described in the section above. Eventually, dielectric layer was printed on the top of silver paths and around pH-sensitive areas to insulate conductive paths from the electrolyte during measurements. Silver conductive layers and GNP/RuO_2 pH-sensitive layers were cured in 120°C for 30 minutes in a chamber dryer. The insulating layers were printed with two different pastes: heat-curable and UV-curable. The former was cured in 120°C for 10 minutes and the latter was cured in UV dryer with the dose around 700 $mJ \cdot cm^{-2}$. All sensor layers were printed with the use of 77T polyester screens. The pH-sensitive layer based on GNP and RuO_2 had a thickness of about 10 μm, the insulating layer of about 20 μm, and silver layer of about 15 μm.

2.4. Measurements. Electrochemical potentials were measured using EMF-16 (Lawson Labs Inc., USA) mV-meter with the following galvanic cell: $Ag/AgCl_{(s)}$, KCl (4M)/bridge electrolyte/sample solution/(RuO_2/GNP/PMMA)/Ag. The bridge electrolyte of the double-junction reference electrode was 1M KCl. Simultaneously, pH of the solution was measured using CP-505 pH-meter (Elmetron, Poland). UV-exposure tests were performed using FC-100/D UV-A (365 nm) lamp (Spectronics Inc., USA). Calibration of the

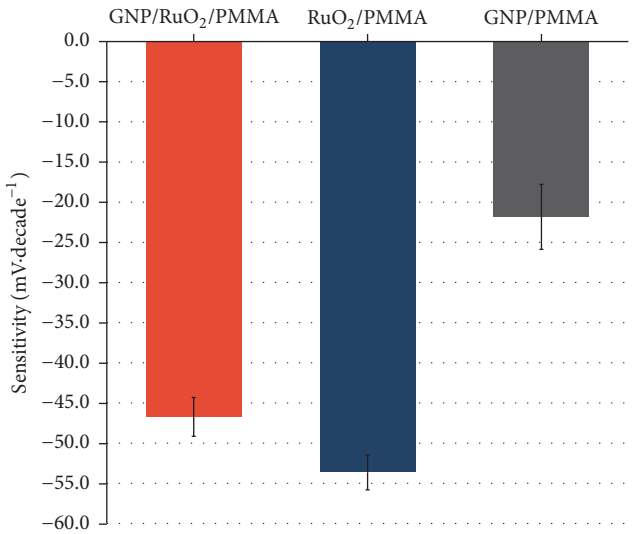

Figure 2: Comparison of the GNP, RuO_2 and GNP/RuO_2-based composites for fabrication of pH sensors.

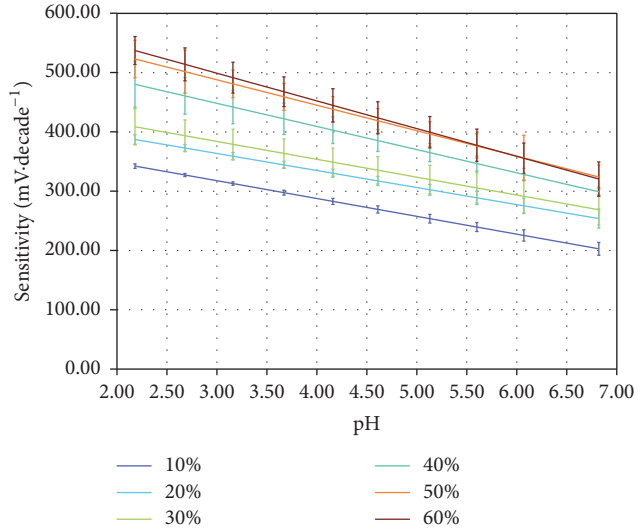

Figure 3: Calibration of the fabricated pH-metric sensors; linear response in pH range 2.18–6.82.

sensors was conducted in 50 mM·L^{-1} citric acid buffer solution with gradually added NaOH solution for pH increment. For each RuO_2 concentration in paste, seven electrodes were calibrated, assuming mean calculated linear regression slope as the sensitivity. Then, calibrated sensors were bent perpendicularly on custom-made bending machine for 10,000 cycles and calibrated again to assess their flexibility.

3. Results and Discussion

3.1. Dependency of Sensitivity on RuO_2 Content. To evaluate applicability of the described composites for pH sensors, calibration of the GNP/PMMA, RuO_2/PMMA, and GNP/RuO_2/PMMA (60 wt% RuO_2) was carried out as described in Section 2.4. Comparison of obtained sensitivity values is shown in Figure 2. As expected, RuO_2/PMMA composite exhibited greater sensitivity than other materials (−53.65 mv·pH^{-1}) and GNP/PMMA the lowest. In GNP/RuO_2/PMMA sensitivity drop was observed, but to verify prospective material costs optimization, influence of the component proportions was further investigated.

Figure 3 shows calibration curves for the sensors prepared as in Sections 2.2 and 2.3. (sensors with UV-curable insulating layer). Linear response of the sensors was observed in pH range of 2.18–6.82. Above this range, next additions of NaOH resulted in buffer solution pH exceeding its linear range. Calculated sensitivity values are presented in Figure 4.

As expected, sensitivity was observed to be the highest for the electrodes with the highest RuO_2 content in paste, although this dependency did not exhibit linear character.

It was observed that, for 10, 20 and 30 wt% of RuO_2 content in the printing paste, sensitivity of the sensors is uniform within margin of error. Above 30 wt%, the value of sensitivity significantly increases (Figure 4). This threshold-like effect was observed more distinctly on logarithmic scale (Figure 5). As it was previously proven when considering conductivity of the printed nanocarbon composites [37, 38],

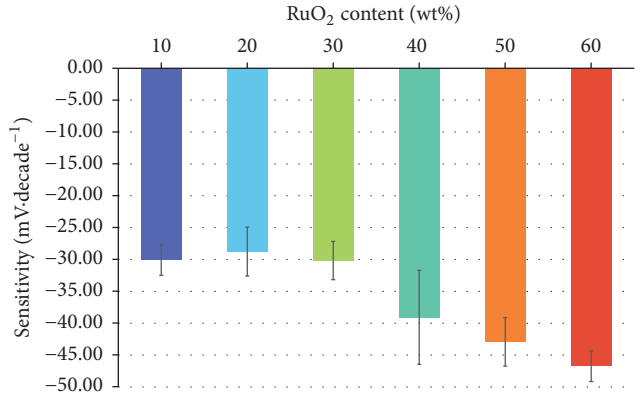

Figure 4: Comparison of the sensitivity calculated for the examined sensors.

some properties of this kind of composites depend on the so-called percolation threshold. According to the percolation theory, properties such as conductivity or permeability are exhibited by a composite only above certain content of the proper phase [39]—in the case of the examined sensors—RuO_2. This threshold can be interpreted as the minimum volume of the RuO_2 in the composite, sufficient to form stable connections with conductive graphene phase which is needed for correct translation of the proton adsorption by RuO_2 to the change of electric potential of the printed electrode.

To determine percolation threshold for sensitivity to pH changes, sensitivity of the 10–30% samples was approximated by the mean value as all the values lie within the same range of confidence (Figure 3). Next, the values obtained for 40–60% samples were used to fit the line in logarithmic scale (Figure 5). Calculated dependency (coefficient of determination R^2 = 97.8%) of sensitivity on RuO_2 wt% content was

$$s = -27.162 \cdot \ln(C) - 58.896, \quad (1)$$

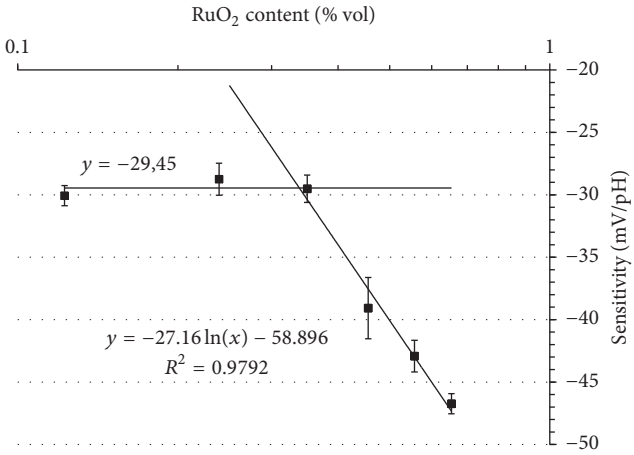

Figure 5: Percolation threshold for sensitivity to pH changes.

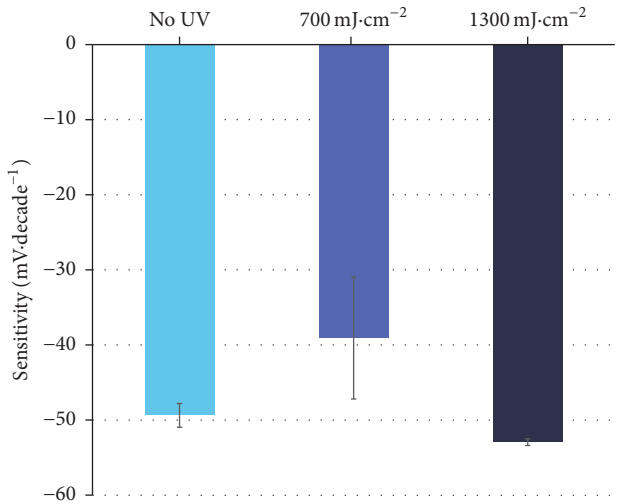

Figure 6: Sensors' sensitivity with respect to the UV exposition.

where s is sensitivity [mV·decade^{-1}] and C is RuO_2 content [vol%].

Thus, the percolation threshold was determined as the cross-section point of the constant sensitivity line and linear increase line. The value obtained from solving (1) was 33.82 vol%.

3.2. Influence of the UV-Irradiation on the Sensors' Performance. As the pH sensing properties of RuO_2 are reported to be strongly influenced by the UV radiation [40] and flexible pH sensors may find application in many fields which implicate exposure to such radiation (e.g., environment monitoring, sport activity tracking, etc.), the dependency of the sensors' indications on this condition was investigated employing sensors with temperature-cured insulating layer and 40 wt% RuO_2 content in paste. Calibration of these sensors was performed as described in Section 2.4 before any exposure to the UV radiation and after irradiation by dose around 1300 mJ·cm^{-2}. Thus, sensitivity values for no UV exposure, 700 and 1300 mJ·cm^{-2} doses, were obtained (Figure 6). Obtained results indicated notably that above certain level of UV exposure the sensitivity increased even above the basic level ($\Delta s = 3.57$ mV·pH^{-1}). It can be explained based on the findings reported in the section above. Since UV radiation is confirmed to cause degradation of PMMA [41, 42], dose high enough to initiate this process may lead to change of the volumetric proportions of the functional material in the electrode layer. Thus, UV-treated sensors fabricated with paste of lower RuO_2 content exhibited higher sensitivity than sensors fabricated with higher RuO_2 content and not exposed to higher doses of UV radiation (50% and 60% samples).

3.3. Flexibility Tests. Performance of the sensors was also tested with respect to their flexibility. Calculated changes of the sensitivity after 10,000 cycles of bending are shown in Table 2. The results may indicate that the number of bending cycles applied is close to the electrodes' material fatigue limit, since the bending caused significant drop in performance in three out of six cases (10%, 20%, and 50% samples). In the case of other samples, the observed increase in sensitivity may derive from the compression of the composite before reaching the fatigue limit, as the compressed composite would be characterized by greater RuO_2 content in the layer's volume (see Section 3.2). This can be observed on the SEM images (Figure 7) of the electrode's surface taken for the sample before (a) and after (b) the bending test. On the SEM image of the sample after bending, there is area of significant RuO_2 particles' thinning. Supposedly, it is due to the fact that cracking of the graphene layer revealed the surface that was not covered by RuO_2 during preparation of the composite paste.

Table 2: Sensors' sensitivity before and after 10,000 cycles of bending.

RuO_2 content [wt%]	Sensitivity [mV·pH^{-1}]		Sensitivity change
	Before	After	
10%	−29.83	−13.14	56.0%
20%	−26.03	−18.82	27.7%
30%	−27.86	−30.41	−9.2%
40%	−46.01	−46.26	−0.5%
50%	−42.90	−34.26	20.1%
60%	−46.17	−50.61	−9.6%

4. Conclusions

Screen printed pH sensors based on the ruthenium (IV) oxide/graphene nanoplatelets composite were fabricated and examined, exhibiting wide linear range (pH 2.18–6.82) and good reproducibility (±5.41% standard deviation for 60% paste). Thresholding effect of the RuO_2 content on sensitivity was observed, which was explained with respect to percolation theory and probability of the RuO_2 connecting with the conductive phase of the composite. Moreover, UV-irradiation was found to influence the sensors' performance positively or negatively, depending on the radiation dose,

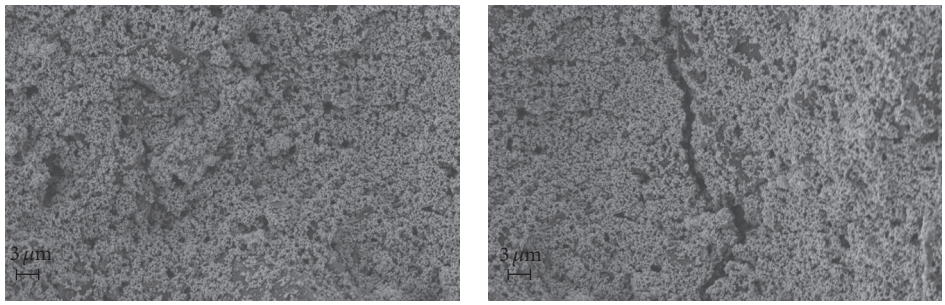

(a) (b)

Figure 7: Comparison of the SEM images of RuO_2/GNP/PMMA composite: before (a) and after (b) bending test.

which also was ascribed to the change in the composite proportions. As the percolation threshold was determined for RuO_2 content and sensitivity-enhancing effect of the UV radiation was observed, this investigation may lead to optimization of the RuO_2 content and thus minimizing the production costs of the sensors. Electrodes were also tested in terms of their flexibility and fatigue resulting in significant performance drop was identified as around 10,000 cycles of perpendicular bending which indicates good endurance for sensors' deformation.

Competing Interests

The authors declare that there is no conflict of interests regarding the publication of this paper.

References

[1] E. B. Secor, B. Y. Ahn, T. Z. Gao, J. A. Lewis, and M. C. Hersam, "Rapid and versatile photonic annealing of graphene inks for flexible printed electronics," *Advanced Materials*, vol. 27, no. 42, pp. 6683–6688, 2015.

[2] Y. H. Jung, T.-H. Chang, H. Zhang et al., "High-performance green flexible electronics based on biodegradable cellulose nanofibril paper," *Nature Communications*, vol. 6, article 7170, 2015.

[3] Z. Wang, W. Wang, Z. Jiang, and D. Yu, "Low temperature sintering nano-silver conductive ink printed on cotton fabric as printed electronics," *Progress in Organic Coatings*, vol. 101, pp. 604–611, 2016.

[4] K. K. Adhikari, Y. Jung, H. Park, G. Cho, and N.-Y. Kim, "Silver-nanoparticle-based screen-printing and film characterization of a disposable, dual-band, bandstop filter on a flexible polyethylene terephthalate substrate," *Journal of Nanomaterials*, vol. 2015, Article ID 810150, 8 pages, 2015.

[5] D. Maddipatla, B. B. Narakathu, S. G. R. Avuthu et al., "A novel flexographic printed strain gauge on paper platform," in *Proceedings of the IEEE SENSORS*, pp. 1–4, IEEE, Busan, South Korea, November 2015.

[6] C. M. Homenick, R. James, G. P. Lopinski et al., "Fully printed and encapsulated SWCNT-based thin film transistors via a combination of R2R gravure and inkjet printing," *ACS Applied Materials & Interfaces*, vol. 8, no. 41, pp. 27900–27910, 2016.

[7] C. Kapnopoulos, E. D. Mekeridis, L. Tzounis et al., "Gravure printed organic photovoltaic modules onto flexible substrates consisting of a P3HT: PCBM photoactive blend," *Materials Today: Proceedings*, vol. 3, no. 3, pp. 746–757, 2016.

[8] T. Laine-Ma, P. Ruuskanen, S. Pasanen, and M. Karttunen, "Pad printing of polymeric silver ink conductors on thermoplastic foils," *Circuit World*, vol. 42, no. 4, pp. 170–177, 2016.

[9] A. Kamyshny and S. Magdassi, "Conductive nanomaterials for printed electronics," *Small*, vol. 10, no. 17, pp. 3515–3535, 2014.

[10] S. Jung, A. Sou, E. Gili, and H. Sirringhaus, "Inkjet-printed resistors with a wide resistance range for printed read-only memory applications," *Organic Electronics: Physics, Materials, Applications*, vol. 14, no. 3, pp. 699–702, 2013.

[11] P. H. Lau, K. Takei, C. Wang et al., "Fully printed, high performance carbon nanotube thin-film transistors on flexible substrates," *Nano Letters*, vol. 13, no. 8, pp. 3864–3869, 2013.

[12] V. Subramanian, J. Chang, and F. Liao, "Printed organic chemical sensors and sensor systems," in *Applications of Organic and Printed Electronics*, pp. 157–177, Springer US, 2013.

[13] N. Matsuhisa, M. Kaltenbrunner, T. Yokota et al., "Printable elastic conductors with a high conductivity for electronic textile applications," *Nature Communications*, vol. 6, 2015.

[14] N. Komoda, M. Nogi, K. Suganuma, H. Koga, and K. Otsuka, "Silver nanowire antenna printed on polymer and paper substrates," in *Proceedings of the 12th IEEE International Conference on Nanotechnology (NANO '12)*, IEEE, Birmingham, UK, August 2012.

[15] A. G. Kelly, D. Finn, A. Harvey, T. Hallam, and J. N. Coleman, "All-printed capacitors from graphene-BN-graphene nanosheet heterostructures," *Applied Physics Letters*, vol. 109, no. 2, Article ID 023107, 2016.

[16] D. Jeschke, M. Niemann, and K. Krüger, "In-situ blending of inkjet-printed thick-film resistors," in *Proceedings of the Additional Conferences (Device Packaging, HiTEC, HiTEN, & CICMT)*, pp. 211–220, September 2013.

[17] G. Wroblewski, K. Kielbasinski, T. Stapinski et al., "Graphene platelets as morphology tailoring additive in carbon nanotube transparent and flexible electrodes for heating applications," *Journal of Nanomaterials*, vol. 2015, Article ID 316315, 8 pages, 2015.

[18] K. Kim, G. Kim, B. R. Lee et al., "High-resolution electrohydrodynamic jet printing of small-molecule organic light-emitting diodes," *Nanoscale*, vol. 7, no. 32, pp. 13410–13415, 2015.

[19] A. Hayat and J. L. Marty, "Disposable screen printed electrochemical sensors: tools for environmental monitoring," *Sensors*, vol. 14, no. 6, pp. 10432–10453, 2014.

[20] S. Mross, T. Zimmermann, N. Winkin, M. Kraft, and H. Vogt, "Integrated multi-sensor system for parallel *in-situ* monitoring

of cell nutrients, metabolites, cell density and pH in biotechnological processes," *Sensors and Actuators, B: Chemical*, vol. 236, pp. 937–946, 2015.

[21] B. Melai, P. Salvo, N. Calisi et al., "A graphene oxide pH sensor for wound monitoring," in *Proceedings of the 38th Annual International Conference of the IEEE Engineering in Medicine and Biology Society (EMBC '16)*, pp. 1898–1901, IEEE, Orlando, Fla, USA, August 2016.

[22] K. S. Johnson, H. W. Jannasch, L. J. Coletti et al., "Deep-Sea DuraFET: a pressure tolerant pH sensor designed for global sensor networks," *Analytical Chemistry*, vol. 88, no. 6, pp. 3249–3256, 2016.

[23] P. Jiang, H. Xia, Z. He, and Z. Wang, "Design of a water environment monitoring system based on wireless sensor networks," *Sensors*, vol. 9, no. 8, pp. 6411–6434, 2009.

[24] L. O'Sullivan, R. P. Ross, and C. Hill, "Potential of bacteriocin-producing lactic acid bacteria for improvements in food safety and quality," *Biochimie*, vol. 84, no. 5-6, pp. 593–604, 2002.

[25] J. Saranya, L. Rajendran, and M. U. Maheswari, "A theoretical model of pH-based potentiometric biosensor based on immobilized enzyme membrane," *American Journal of Analytical Chemistry*, vol. 7, no. 4, pp. 363–377, 2016.

[26] E. M. McConnell, R. Bolzon, P. Mezin, G. Frahm, M. Johnston, and M. C. DeRosa, "PHAST (pH-Driven Aptamer Switch for Thrombin) Catch-and-Release of Target Protein," *Bioconjugate Chemistry*, vol. 27, no. 6, pp. 1493–1499, 2016.

[27] E. Voitechovic, D. Kirsanov, and A. Legin, "An approach to potentiometric sensing of sugars: Baker's yeast assisted pH electrode," *Sensors and Actuators, B: Chemical*, vol. 225, pp. 209–212, 2016.

[28] G. Wróblewskia, M. Słomaa, D. Janczak, A. Młozniakb, and M. Jakubowska, "Influence of carbon nanoparticles morphology on physical properties of polymer composites," *Acta Physica Polonica A*, vol. 125, no. 4, pp. 861–863, 2014.

[29] P. Kurzweil, "Metal oxides and ion-exchanging surfaces as pH sensors in liquids: state-of-the-art and outlook," *Sensors*, vol. 9, no. 6, pp. 4955–4985, 2009.

[30] P. Kurzweil, "Precious metal oxides for electrochemical energy converters: pseudocapacitance and pH dependence of redox processes," *Journal of Power Sources*, vol. 190, no. 1, pp. 189–200, 2009.

[31] S. Al-Hilli and M. Willander, "The pH response and sensing mechanism of n-type ZnO/electrolyte interfaces," *Sensors*, vol. 9, no. 9, pp. 7445–7480, 2009.

[32] M. Chen, Y. Jin, X. Qu, Q. Jin, and J. Zhao, "Electrochemical impedance spectroscopy study of Ta_2O_5 based EIOS pH sensors in acid environment," *Sensors and Actuators B: Chemical*, vol. 192, pp. 399–405, 2014.

[33] L. A. Pocrifka, C. Gonçalves, P. Grossi, P. C. Colpa, and E. C. Pereira, "Development of RuO_2-TiO_2 (70–30) mol% for pH measurements," *Sensors and Actuators, B: Chemical*, vol. 113, no. 2, pp. 1012–1016, 2006.

[34] N. Lei, P. Li, W. Xue, and J. Xu, "Simple graphene chemiresistors as pH sensors: fabrication and characterization," *Measurement Science and Technology*, vol. 22, no. 10, Article ID 107002, 2011.

[35] P. K. Ang, W. Chen, A. T. S. Wee, and P. L. Kian, "Solution-gated epitaxial graphene as pH sensor," *Journal of the American Chemical Society*, vol. 130, no. 44, pp. 14392–14393, 2008.

[36] L. Manjakkal, K. Cvejin, J. Kulawik, K. Zaraska, D. Szwagierczak, and R. P. Socha, "Fabrication of thick film sensitive RuO_2-TiO_2 and Ag/AgCl/KCl reference electrodes and their application for pH measurements," *Sensors and Actuators, B: Chemical*, vol. 204, pp. 57–67, 2014.

[37] X. Wu, S. Qi, J. He, and G. Duan, "High conductivity and low percolation threshold in polyaniline/graphite nanosheets composites," *Journal of Materials Science*, vol. 45, no. 2, pp. 483–489, 2010.

[38] K. Kalaitzidou, H. Fukushima, and L. T. Drzal, "A new compounding method for exfoliated graphite-polypropylene nanocomposites with enhanced flexural properties and lower percolation threshold," *Composites Science and Technology*, vol. 67, no. 10, pp. 2045–2051, 2007.

[39] S. R. Broadbent and J. M. Hammersley, "Percolation processes: I. Crystals and mazes," *Mathematical Proceedings of the Cambridge Philosophical Society*, vol. 53, no. 3, pp. 629–641, 1957.

[40] Y.-H. Liao and J.-C. Chou, "Preparation and characteristics of ruthenium dioxide for pH array sensors with real-time measurement system," *Sensors and Actuators, B: Chemical*, vol. 128, no. 2, pp. 603–612, 2008.

[41] S. Eve and J. Mohr, "Study of the surface modification of the PMMA by UV-radiation," *Procedia Engineering*, vol. 1, no. 1, pp. 237–240, 2009.

[42] T. Çaykara and O. Güven, "UV degradation of poly(methyl methacrylate) and its vinyltriethoxysilane containing copolymers," *Polymer Degradation and Stability*, vol. 65, no. 2, pp. 225–229, 1999.